

PERFORMANCE OF TWO DIFFERENT HIGH-ACCURACY UPWIND SCHEMES IN INVISCID COMPRESSIBLE FLOW FIELDS

R. Hosseini^{1*}, M.H. Rahimian² and M. Mirzaei³

Performance of first, second and third order accurate methods for calculation of inviscid fluxes in fluid flow governing equations are investigated here. For the purpose, an upwind method based on Roe's scheme is used to solve 2-dimensional Euler equations. To increase the accuracy of the method two different schemes are applied. The first one is a second and third order upwind-based algorithm with the MUSCL extrapolation Van Leer (1979), based on primitive variables. The other one is an upwind-based algorithm with the Chakravarthy extrapolation to the fluxes of mass, momentum and energy. The results show that the thickness of shock layer in the third order accuracy is less than its value in second order. Moreover, applying limiter eliminates the oscillations near the shock while increases the thickness of shock layer especially in MUSCL method using Van Albada limiter.

Keywords: Euler, Roe, High-Accuracy, MUSCL, Chakravarthy

1. INTRODUCTION

The history of numerical techniques for the resolution of inviscid Euler equations goes back to the early 1950s, with the first order method of Courant et al.[1], and Lax and Friedrichs.[2] The second order accurate Lax-Wendroff has led to a whole family of variants when applied to non-linear systems.[3] MacCormack method was one of the most popular of these variants.[4] Space-centered schemes of second order accuracy in space were initially introduced with implicit linear multi-step time integration methods by Brily and McDonald, [5] and Beam and Warming.[6] Due to the unwanted oscillations that are created in central algorithms, upwind schemes were introduced to prevent these oscillations. The first explicit upwind scheme was introduced by Courant et al. (1952).[1] Steger and Warming[7] and Van Leer[8] introduced the flux vector splitting as member of upwind group.

The other subgroup of this method was introduced by Godonov (1959)[9] which is based on the exact solution of Reimann problem. This most original approach has generated a series of schemes that introduce different approximation Reimann solver. The most important solution of these schemes has been introduced by Osher, 1982[10]; Roe, 1981.[11] In this paper the upwind Roe's scheme has been used to solve two-dimensional Euler equation in curvilinear coordinate system. To increase the accuracy of the results Chakravarthy and MUSCL methods have been used for extrapolation of properties. To prevent the generation of oscillations near discontinuities Minmod or Van Albada limiters are used in the above methods.

2. GOVERNING EQUATIONS

The governing equations of fluid motion for two-dimensional, unsteady, compressible flow in full conservative form with no body force can be written as[12]:

$$\frac{\partial \bar{Q}}{\partial t} + \frac{\partial \bar{E}}{\partial \xi} + \frac{\partial \bar{F}}{\partial \eta} = 0 \quad (1)$$

where \bar{Q} , solution vector, and \bar{E}, \bar{F} , inviscid flux

Received: July 21, 2004, Accepted: February 19, 2005.

1 Graduate School, Mechanical Eng. Department, Faculty of Eng., University of Tehran, Tehran, Iran

2 Mechanical Eng. Department, Faculty of Eng., University of Tehran, Tehran, Iran

3 Mechanical Eng. Department, K.N.Toosi University of Technology, Tehran, Iran

* Corresponding author. E-mail: hoseeinis@me.ut.ac.ir

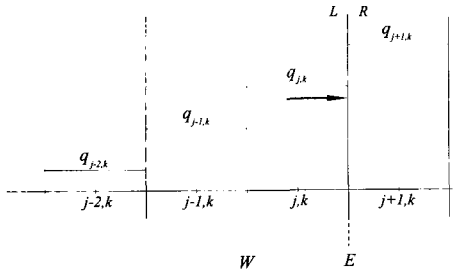


Fig. 1 The cell face value L is determined by the first order upwinding[13]

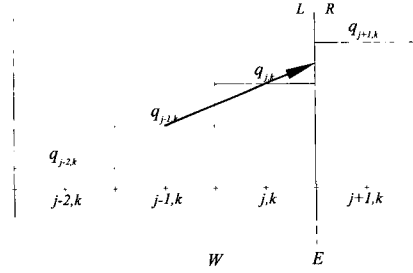


Fig. 2 The cell face value L is determined by the second order upwinding[13]

vectors in ξ, η directions respectively, are:

$$\begin{aligned} \bar{Q} &= \frac{Q}{J}, \quad \bar{E} = \frac{1}{J} [\xi_x E + \xi_y F] \\ \bar{F} &= \frac{1}{J} [\eta_x E + \eta_y F] \end{aligned} \quad (2)$$

Q, E, and F are:

$$\begin{aligned} Q &= [\rho \quad \rho u \quad \rho v \quad E_t]^T \\ E &= [\rho u \quad \rho u^2 + p \quad \rho uv \quad (E_t + p)u]^T \\ F &= [\rho v \quad \rho uv \quad \rho v^2 + p \quad (E_t + p)v]^T \end{aligned}$$

and ρ, p, u, v, E_t are density, pressure, x- and y-velocity component, and the total energy per unit volume, respectively. For a calorically perfect gas, pressure is estimated by the equation of state:

$$p = \rho(\gamma - 1)e$$

where γ is the ratio of specific heats.

3. DISCRETIZATION

The governing equations are discretized in a structural grid using finite volume technique and for time discretization, a simple explicit scheme is applied. The discretized form of the equations in a computational cell is as follow:

$$\frac{\bar{Q}_{i,j}^{n+1} - \bar{Q}_{i,j}^n}{\Delta\tau} + \frac{\bar{E}_{i+\frac{1}{2},j}^n - \bar{E}_{i-\frac{1}{2},j}^n}{\Delta\xi} + \frac{\bar{F}_{i,j+\frac{1}{2}}^n - \bar{F}_{i,j-\frac{1}{2}}^n}{\Delta\eta} = 0 \quad (3)$$

4. Numerical Method

As stated previously, in this study upwind Roe's scheme is used to solve two-dimensional inviscid Euler equations. The flow conditions (L) and (R) at the cell interface (E) can be determined in accordance with the degree of accuracy and type of scheme.

The first order upwind algorithm suggests that:

$$q_E^L = q_{j,k} \quad q_E^R = q_{j+1,k}$$

where q is a typical primitive variable, i.e. $q \in \{\rho, p, u, v\}$. For the first order extrapolation a zero-polynomial (a straight flat line) is used to extrapolate the primitive variable q at node (j,k) to the cell face E. (Fig. 1)

4.1 MUSCL METHOD

In this computation a second and third order algorithm with the extrapolation strategy of Van Leer (1979)[14], is applied to primitive variables pressure (p), velocity components (u, v) and temperature (T), in order to obtain the inner (L) and outer (R) flow conditions.

Second order upwinding recommends:

$$\begin{aligned} q_E^L &= q_{j,k} + \frac{1}{2} \Delta_W q \\ q_E^R &= q_{j+1,k} - \frac{1}{2} \Delta_{EE} q \end{aligned}$$

where $\Delta_W q$ and $\Delta_{EE} q$ are the jump of a primitive variable at the west and east face of the control volume, i.e.

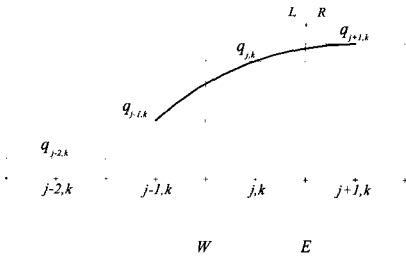


Fig. 3 The cell face value L as determined by the third order upwind-biased extrapolation[13]

$$\Delta_w q = (q_{j,k} - q_{j-1,k})$$

$$\Delta_{EE} q = (q_{j+2,k} - q_{j+1,k})$$

For the second order extrapolation a first-order polynomial, i.e. a straight line, is used to extrapolate the primitive variable q from the nodes (j-1,k) and (j,k) to the cell face E, as shown in Fig. 2.

A third order upwind-biased algorithm proposes:

$$q_E^L = q_{j,k} + \frac{1}{4}[(1-k)\Delta_w q + (1+k)\Delta_E q],$$

$$q_E^R = q_{j+1,k} - \frac{1}{4}[(1-k)\Delta_{EE} q + (1+k)\Delta_E q]$$

where $k = \frac{1}{3}$ and $\Delta_E q = q_{j+1,k} - q_{j,k}$

It is noted that for the third order extrapolation a second-order polynomial, i.e. a parabola, is used as shown in Fig. 3. That is a second order polynomial curve fit between the points (j-1,k), (j,k) and (j+1,k) used to obtain q_E^L .

Van Albada limiter-In the higher order methods, i.e. higher than first order accurate cases, the solution is not necessarily monotonous and non-physical oscillations are produced, which must be damped. To damp the numerical oscillations, in the current computations, the Van Albada et. al. flux limiter (1982)[15], is applied. The approach as implemented here is:

$$q_E^L = q_{j,k} + \frac{\phi}{4}[(1-k)\Delta_w q + (1+k)\Delta_E q]$$

$$q_E^R = q_{j+1,k} - \frac{\phi}{4}[(1-k)\Delta_{EE} q + (1+k)\Delta_E q]$$

where ϕ is the limiter function, which is a function of forward- and backward-differences, as defined by:

$$\phi_{j,k} \equiv \frac{2(\Delta_w q)(\Delta_E q) + \epsilon}{(\Delta_w q)^2 + (\Delta_E q)^2 + \epsilon}$$

and ϵ is a small number which prevents indeterminacy in regions of uniform flow, i.e. in region $(\Delta_w q) = (\Delta_E q) = 0$.

4.2 CHAKRAVARTHY METHOD

In this method, a family of scheme is presented based on the preprocessing approach.[16] Some convenient variables are now defined as an intermediate step before defining the numerical flux corresponding to a high-accuracy TVD scheme. First, parameters denoted as α are defined. These provide a measure of the change in dependent variables across the corresponding wave family and therefore measure the slope between neighboring states. In the following, the superscript i corresponds, as usual, to the ith eigenvalue and ith eigenvector. The subscripts 1-3 are just labels to differentiate between the three different types of α parameters[17].

$$\alpha_{1,m+\frac{1}{2}}^i = l_{m+\frac{1}{2}}^i (Q_m - Q_{m-1})$$

$$\alpha_{2,m+\frac{1}{2}}^i = l_{m+\frac{1}{2}}^i (Q_{m+1} - Q_m)$$

$$\alpha_{3,m+\frac{1}{2}}^i = l_{m+\frac{1}{2}}^i (Q_{m+2} - Q_{m+1})$$

where l is the orthonormal set of left eigenvector corresponding to a cell face. Next, the slope-limited values are defined by:

$$\tilde{\alpha}_{1,m+\frac{1}{2}}^i = \min \text{mod}[\alpha_{1,m+\frac{1}{2}}^i, b\alpha_{2,m+\frac{1}{2}}^i]$$

$$\tilde{\alpha}_{2,m+\frac{1}{2}}^i = \min \text{mod}[\alpha_{2,m+\frac{1}{2}}^i, b\alpha_{1,m+\frac{1}{2}}^i]$$

$$\tilde{\alpha}_{2,m+\frac{1}{2}}^i = \min \text{mod}[\alpha_{2,m+\frac{1}{2}}^i, b\alpha_{3,m+\frac{1}{2}}^i]$$

$$\tilde{\alpha}_{3,m+\frac{1}{2}}^i = \min \text{mod}[\alpha_{3,m+\frac{1}{2}}^i, b\alpha_{2,m+\frac{1}{2}}^i]$$

In the above, the compression parameter b is to

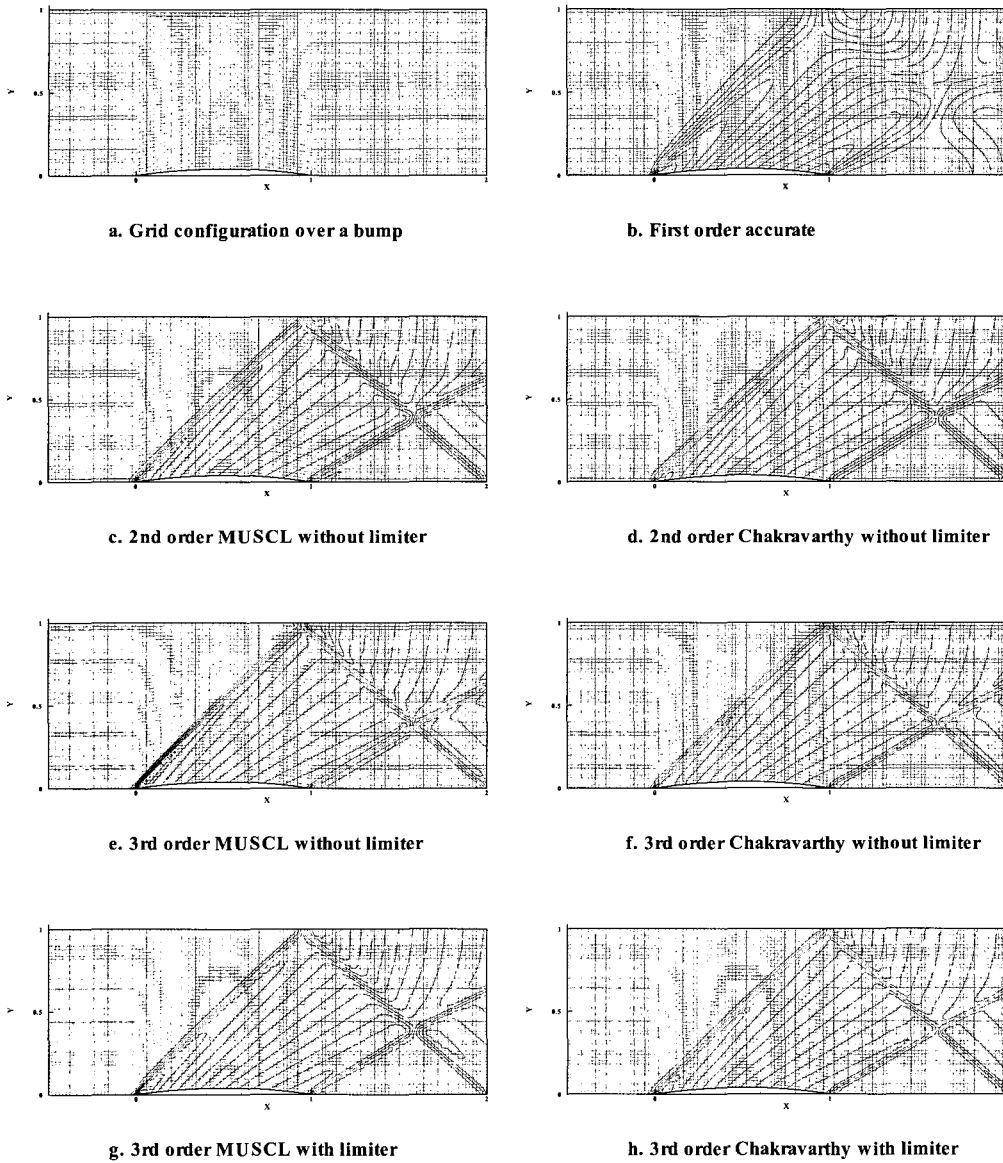


Fig. 4 Pressure contours of supersonic flow over a bump with inlet Mach number of 1.65

be taken as the following function of the accuracy parameter ϕ , which is explained shortly.

$$b = (3 - \phi)/(1 - \phi)$$

The **Minmod slope-limiter** operator is[14]:

$$\text{Mimmod}[x,y]= \text{Sign}(x) \max[0, \min\{|x|, y\text{sign}(x)\}]$$

In equations (2), numerical fluxes \bar{E}, \bar{F} were introduced. Based on the concise notation of using f to represent either \bar{E} or \bar{F} , let us use \bar{f} to denote the numerical fluxes \bar{E} or \bar{F} . A family of TVD schemes can be written down as follows in terms of the previously defined α parameters (with the subscript $m + \frac{1}{2}$ dropped from these for convenience):

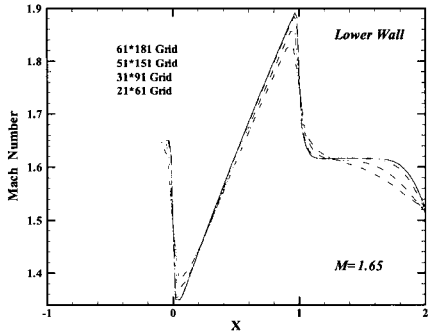


Fig. 5 Distribution of Mach number on the lower wall in different grid

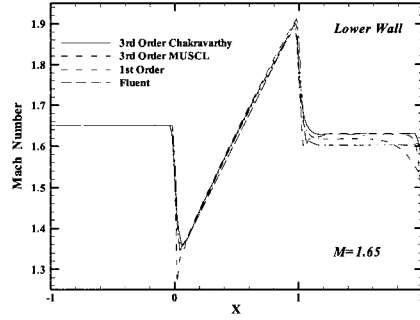


Fig. 7 Distribution of Mach number on the lower wall in different accuracy

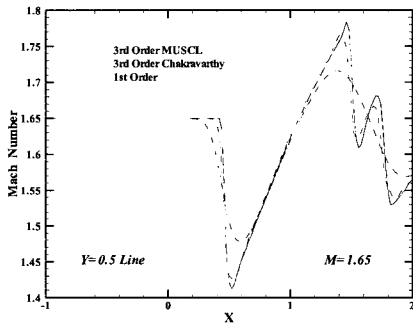


Fig. 6 Distribution of Mach number along the middle line of channel(Y=0.5)

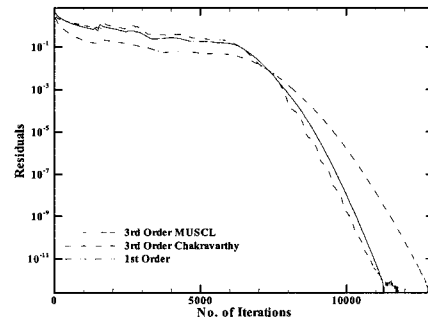


Fig. 8 Residuals history

$$\begin{aligned} \bar{f}_{m+\frac{1}{2}} &= h_{m+\frac{1}{2}} \\ &+ \sum_i \left(\frac{1+\phi}{4} \tilde{\alpha}_2^i + \frac{1-\phi}{4} \tilde{\alpha}_1^i \right) \lambda_{m+\frac{1}{2}}^{i+} r_{m+\frac{1}{2}}^i \\ &- \sum_i \left(\frac{1+\phi}{4} \tilde{\alpha}_2^i + \frac{1-\phi}{4} \tilde{\alpha}_3^i \right) \lambda_{m+\frac{1}{2}}^{i+} r_{m+\frac{1}{2}}^i \end{aligned} \quad (5)$$

where λ, r are eigenvalue and right eigenvector, respectively.

The first term on the right-hand side of equation (5) defines a first-order numerical flux and is constructed from:

$$\begin{aligned} h_{m+\frac{1}{2}} &= \frac{1}{2} [f(Q_{m+\frac{1}{2}}, N_{m+\frac{1}{2}}) \\ &+ f(Q_m, N_{m+\frac{1}{2}})] \\ &- \frac{1}{2} \left[\sum_i (\lambda_{m+\frac{1}{2}}^{i+} - \lambda_{m+\frac{1}{2}}^{i-}) \alpha_2^i r_{m+\frac{1}{2}}^i \right] \end{aligned} \quad (6)$$

The parameter ϕ defines schemes of varying accuracy. The notations $\tilde{\alpha}^i$ and $\tilde{\alpha}^i$ have been used to define slope-limited values of the α parameters. If these are replaced by their unlimited values, the truncation error of the resulting schemes (in one-dimensional steady-state problems on uniform grids) is given by:

$$TE = -\left(\frac{\phi - 1/3}{4}\right) (\Delta x)^2 \frac{\partial f}{\partial Q} \frac{\partial^3 Q}{\partial x^3}$$

Here, the truncation error refers to the difference between the centroidal value of the numerical solution and the average value of the exact solution in that cell. The choice of $\phi=1/3$ results in a TVD scheme based on an underlying third-order scheme. The choice of $\phi=-1$ results in a TVD scheme

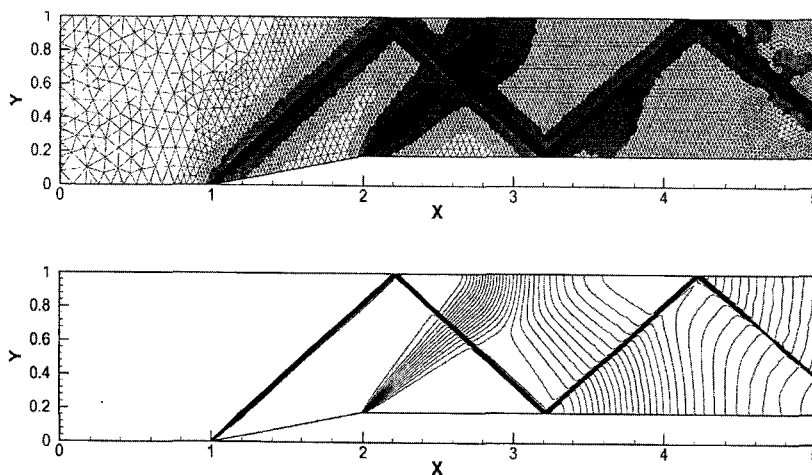


Fig. 9 Pressure contours in unstructured adaptive mesh refinement domain[18]

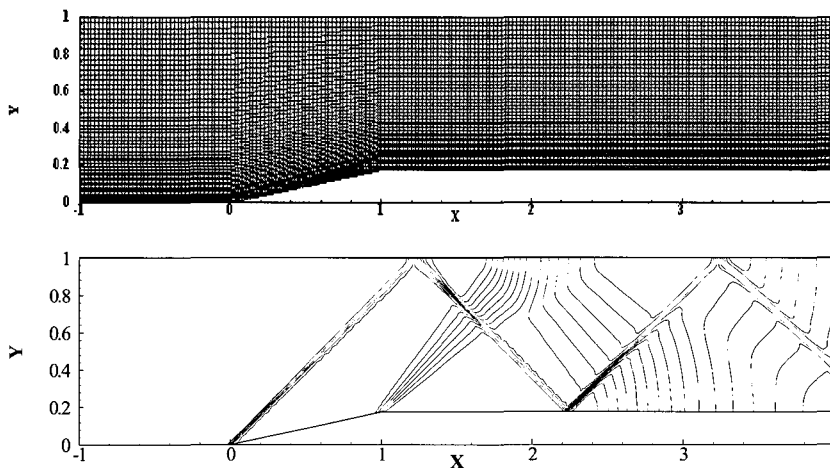


Fig. 10 Pressure contours in structured mesh with 3rd order Chakravarthy method

based on the fully upwind second-order-accurate formulation.

5. RESULTS AND DISCUSSION

To indicate performance of the presented schemes, two various test cases are analyzed. The first test case is a supersonic inviscid flow with Mach number of 1.65 over a 4% bump and second one is a supersonic flow with Mach number of 2.0 over a 10-degree compression corner.

To show the reliability of the code, Mach number distribution along the bottom wall of the bump domain for 21x61, 31x91, 51x151 and 61x181 grids

are compared and grid independency of the code is achieved (Fig. 5). The code is run on a 1.5 GHz. Pentium 4 computer and run time for 51 x 151 grids is about 20 minutes.

The results of the test cases are shown in Figs. 4 to 11. For the first case Fig. 4-a shows 51x151 grids in physical domain. The pressure contours in the domain for first, second and third order accurate methods are indicated in Figs. 4-b to 4-h by using MUSCL and Chakravarthy extrapolation. As seen in Fig. 4-b, the first order accuracy method cannot capture the shocks accurately and especially the reflections while in the second and third order (Figs. 1-c to 1-f) the discontinuities are

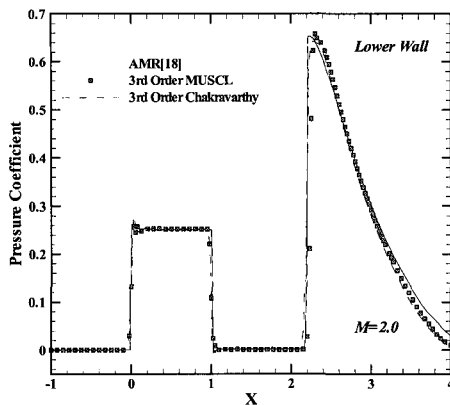


Fig 11 Pressure distribution on the lower wall of compression corner

captured completely. Comparison of Figs. 4-c, 4-d with Figs. 4-e, 4-f, shows that the third order accuracy shock layer thickness is less than its value in second order. Also, the comparison of Fig. 4-e and 4-g, represents applying limiter eliminates the oscillations near the shock while increases the thickness of shock layer in both methods. Of course, the increase in MUSCL scheme is noticeable but in Chakravarthy method is almost negligible.

It is needed to explain that, Chakravarthy method uses extrapolation of the convective fluxes. Obviously, convective fluxes are variation of primitive variables. Near discontinuities, oscillations of variables increase and it causes increase in total variation of primitive variables. Minmod limiter controls the slope of the variables to eliminate oscillations near discontinuities. The elimination of oscillations does not change the thickness of the shock. In MUSCL method, extrapolation of primitive variables, instead of their variations, is used to obtain variables at the cell surface. In this method oscillations appear near discontinuities too. By using Van Albada limiter it is to eliminate these oscillations. Van Albada limiter uses a weighting function equation, for extrapolation of primitive variables at the left and right of the cell surface.

In Fig. 6, distribution of Mach number along the middle of channel ($Y=0.5$) is shown. As it was anticipated, contrary to the first order method that couldn't capture reflected shock precisely, the third order schemes captured reflection of the shock perfectly. The profile of Mach number on the lower

wall of the duct with the same geometry is indicated in Fig. 7. First, second and third order accuracies in the above methods are compared and the results shows a highly conformity with those of literature. The residuals of the methods are shown in the Fig. 8. It is seen that the residuals drop to machine accuracy.

The second test case geometry, a compression corner, is indicated in Fig. 9 and 10. The pressure contours of a supersonic flow in an unstructured flow field are shown in Fig. 9 using adaptive mesh refinement method (AMD)[18], while Fig. 10 presents the contours in a structure flow field applying Chakravarthy method.

The profile of pressure coefficient at the lower wall of a compression corner is plotted in Fig. 11, using Chakravarthy and MUSCL methods with Mach number of 2.0. As observed the results are well agreed with those of AMD. It seems that, Chakravarthy method with or without limiter, in comparison with MUSCL scheme, not only have better shock capturing capability, but also have a superior pressure and Mach number profile, in this Mach number limit.

6. CONCLUSIONS

In the above study Roe's upwind algorithm is used to solve two-dimensional Euler equations in a supersonic compressible flow field. Two different high-accuracy extrapolations, Chakravarthy and MUSCL, are applied to increase the accuracy of the method. The results show that unlike the first order accuracy method, the second and third order accuracy schemes can capture the shock and its reflection perfectly. Comparison of the outcomes indicate the Chakravarthy method have a better ability of shock capturing than MUSCL scheme especially when the limiters are applied.

ACKNOWLEDGEMENT

The authors would like to thank Dr. Mohammad Jafar Kermani for his honest help during this study.

REFERENCES

- [1] Courant, R., Isaacson, E. and Reeves, M., 1952, "On the solution of nonlinear hyperbolic differential equations by finite differences,"

- Comm. Pure and Applied Mathematics*, Vol.5, pp.243-55.
- [2] Lax, P.D., 1954, "Weak solutions of nonlinear hyperbolic equations and their numerical computation," *Comm Pure and Applied Mathematics*, Vol.7, pp.159-93.
- [3] Lax, P.D. and Wendroff, B., 1964, "Difference schemes for hyperbolic equations with high order of accuracy," *Comm Pure and Applied Mathematics*, Vol.17, pp.381-98.
- [4] MacCormack, R.W., 1969, "The effect of viscosity in hypervelocity impact cratering," *AIAA*, pp.69-354.
- [5] Briley, W.R. and McDonald, H., 1975, "Solution of the three-dimensional Navier-Stokes equations by an implicit technique," *Proc. Fourth International Conference on Numerical Methods in Fluid Dynamics*, Lecture Notes in Physics, Vol.35, Berlin: Springer.
- [6] Beam, R.M. and Warming, R.F., 1976, "An implicit finite-difference algorithm for hyperbolic system in conservation law form," *Journal Computational Physics*, Vol.22, pp.87-109.
- [7] Steger, J.L. and Warming, R.F., 1981, "Flux vector splitting of the inviscid gas-dynamic equations with application to finite difference methods," *Journal Computational Physics*, Vol.40, pp.263-93.
- [8] Van Leer, B., 1982, "Flux vector splitting for the Euler equations," *In Proc. 8th International Conference on Numerical Methods in Fluid Dynamics*, Springer Verlag.
- [9] Godunov, S.K., 1959, "A difference scheme for numerical computation of discontinuous solution of hydrodynamic equations," *Math. Sbornik*, Vol.47, pp.271-300 (in Russian). Translated US Joint Publ. Res. Service, JPRS 7226.
- [10] Osher, S., 1984, "Riemann solvers, the entropy condition and difference approximations," *SIAM Journal Numerical Analysis*, Vol.21, pp.217-35.
- [11] Roe, P.L., 1981, "Approximate Riemann solvers, parameter vectors and difference schemes," *Journal Computational Physics*, Vol.43, pp.357-72.
- [12] Hirsch, C., 1990, *Numerical Computation of Internal and External Flows*, Vol.2, Wiley, New York.
- [13] Kermani, M.J., 2001, "Development and Assessment of Upwind Schemes with Application to Inviscid and Viscous Flows on Structured Meshes," *PhD thesis*, Carleton University, Canada.
- [14] Van Leer, B., 1979, "Towards the Ultimate Conservation Difference Scheme, V, A Second Order Sequel to Godunov's Method," *Journal Comput. Phys.*, Vol.32, pp.110-136.
- [15] Van Albada, G.D., Van Leer, B. and Roberts, W.W., 1982, "A Comparative Study of Computational Methods in Cosmic Gas Dynamics," *Astron. Astrophys.*, Vol.108, pp.76-84.
- [16] Chakravarthy, S.R. and Osher, S., 1985, "Computing With High-Resolution Upwind Schemes for Hyperbolic Equations," *Lectures in Applied Mathematics*, Vol.22, American Mathematical Society, pp.57-86.
- [17] Chakravarthy, S.R. and Szema, K.Y., 1987, "Euler Solver for Three Dimensional Supersonic Flows with Subsonic Pockets" *J.Aircraft*, Vol.24, No.2, pp.73-83.
- [18] Ripley, R.C., Lien, F.-S. and Yovanovich, M.M., 2002, "Isotropic Mesh Adaption of Supersonic Channel Flows on Unstructured Meshes," *Proceeding of CFD 2002 Conference*, Windsor, Canada, pp.311-316.